ChemPubSoc Europe

DOI: 10.1002/cbic.201402715

CHEMBIOCHEM Full Papers

Bioorthogonal Probes for Imaging Sterols in Cells

Cindy Y. Jao,[a] Daniel Nedelcu,[a] Lyle V. Lopez,[a] Thilani N. Samarakoon,[b] Ruth Welti,[b] and Adrian Salic*[a]

Cholesterol is a fundamental lipid component of eukaryotic membranes and a precursor of potent signaling molecules, such as oxysterols and steroid hormones. Cholesterol and oxysterols are also essential for Hedgehog signaling, a pathway critical in embryogenesis and cancer. Despite their importance, the use of imaging sterols in cells is currently very limited. We introduce a robust and versatile method for sterol microscopy based on C_{19} alkyne cholesterol and oxysterol analogues. These sterol analogues are fully functional; they rescue growth of cholesterol auxotrophic cells and faithfully recapitulate the multiple roles that sterols play in Hedgehog signal transduction. Alkyne sterol analogues incorporate efficiently into cellular membranes and can be imaged with high resolution after copper(I)-catalyzed azide–alkyne cycloaddition reaction with fluorescent azides. We demonstrate the use of alkyne sterol probes for visualizing the subcellular distribution of cholesterol and for two-color imaging of sterols and choline phospholipids. Our imaging strategy should be broadly applicable to studying the role of sterols in normal physiology and disease.

Introduction

Cholesterol (Chol) plays important structural and regulatory functions in eukaryotic membranes,[1] and its cellular levels are tightly controlled by complex mechanisms that regulate its synthesis, uptake, distribution, and elimination.[2] By modulating the physical properties of phospholipid bilayers and through their interaction with membrane proteins, Chol has a broad impact on a large number of cellular processes. Chol is also a metabolic precursor of oxysterols and steroid hormones, which have potent effects on cell signaling, metabolism, and gene expression. Finally, sterols have emerged as playing critical roles in Hedgehog (Hh) signaling, a pathway involved in many aspects of embryonic development, adult stem cell maintenance, and multiple human cancers.[3] Sterols are important for three essential steps in Hh signaling: 1) Chol is covalently attached to the Hh ligand in the signaling cell,[4] a modification critical for proper Hh signaling; defects in Chol attachment to the Hh ligand cause holoprosencephaly, one of the most frequent congenital malformations of the central nervous system.[5] 2) In vertebrates, Chol is required for activation of the seven-spanner membrane protein Smoothened (Smo)[6] and, thus, for Hh signal transduction in the responding cell;[7] this requirement has been proposed to underlie the defective Hh signaling seen in inborn errors of cholesterol synthesis. 3) Oxysterols bind and activate vertebrate Smo,[8] an interaction required for normal Hh signaling.[9]

Contrasting the importance of sterols in biology, the methods currently available for microscopic imaging of these compounds in cells are few and often suffer from major limitations. One sterol imaging approach uses fluorescent derivatives of Chol in which a fluorophore moiety (such as NBD or BODIPY) replaces part of the isooctyl tail[10] or is attached to the 3β-OH group;[11] these derivatives are problematic, because the bulky fluorophores perturb critical structural elements of the Chol molecule. Another approach makes use of Chol analogues with conjugated double bonds that display intrinsic fluorescence, such as cholestatrienol[12] or dehydroergosterol.[13] These sterols are good Chol mimics but have poor fluorescence characteristics (low extinction coefficients and photostability) and absorb at short wavelengths, where cellular autofluorescence and phototoxicity are high. Alternatively, Chol can be visualized indirectly, by using fluorescent polyene macrolide antibiotics that bind Chol, such as filipin and nystatin;[14] this method is prone to artifacts and is limited by the poor fluorescence properties of these molecules (low extinction coefficients, poor photostability, and short excitation wavelengths). These indirect methods for cholesterol detection have been further refined to improve probe photostability. One strategy employs fluorescent conjugates of theonellamides,[15] bicyclic peptides isolated from marine sponges that bind cholesterol. Another approach for imaging cholesterol uses biotinylated perfringolysin O,[16] a secreted bacterial cytolitic protein that binds membranes in a cholesterol-dependent manner. Finally, (25*R*)-25-ethynyl-26-nor-3β-hydroxycholest-5-en (alkyne cholesterol), a recently described cholesterol analogue,[17] can be visualized following copper(I)-catalyzed azide–alkyne cycloaddition (CuAAC)[18] with a fluorescent azide. In alkyne cholesterol, an ethynyl group replaces the C-26 methyl in the isooctyl tail.

[a] *Dr. C. Y. Jao, Dr. D. Nedelcu, Dr. L. V. Lopez, Prof. Dr. A. Salic*
Department of Cell Biology, Harvard Medical School
240 Longwood Avenue, Boston, MA 02115 (USA)
E-mail: asalic@hms.harvard.edu

[b] *Dr. T. N. Samarakoon, Prof. Dr. R. Welti*
Kansas Lipidomics Research Center, Division of Biology
Kansas State University
Manhattan, KS 66506 (USA)

Supporting information for this article is available on the WWW under http://dx.doi.org/10.1002/cbic.201402715: detailed experimental procedures, synthetic methods, chemical compound information, and supplementary results.

As the tail of cholesterol projects into the interior of the membrane bilayer, it is unclear how a fluorescent azide might gain access to the ethynyl group of a membrane-embedded alkyne cholesterol molecule.

To develop an improved method to image sterols in cells, we first synthesized 19-ethynylcholesterol (eChol), a Chol analogue containing an ethynyl group instead of the axial methyl group at the C-19 position of the Chol molecule. EChol can completely replace Chol in supporting the growth of Chol auxotrophic cells, demonstrating that eChol closely mimics the biological properties of Chol. Furthermore, eChol is an efficient substitute for Chol in the Hh pathway, both in processing and in Chol modification of the Hh ligand, and in satisfying the Chol requirement for Hh signal transduction at the level of Smo. We extended our alkyne tagging strategy to oxysterols by synthesizing the 19-ethynyl derivative of 25-hydroxycholesterol (25-OH-eChol), an oxysterol analogue that we show recapitulates the potent stimulatory effects of oxysterols on the vertebrate Hh pathway. When added to cells, eChol and 25-OH-eChol partition efficiently into cellular membranes and can be imaged by high-resolution fluorescence microscopy following derivatization with a fluorescent azide through CuAAC. Our strategy for imaging Chol and oxysterols has several advantages over other available techniques and should facilitate imaging studies of the role of sterols in various cellular processes under both normal and pathological conditions.

Results and Discussion

To develop a chemical strategy for visualizing Chol in cells, we synthesized the alkyne analogue 19-ethynylcholesterol (eChol; Figure 1A). We chose to introduce the ethynyl group at the C-19 position of the Chol molecule for the following reasons: 1) synthetic accessibility: the C-19 position has been derivatized in many sterols and steroids;[19] 2) steric accessibility: to visualize the Chol analogue by CuAAC reaction with fluorescent azides, the alkyne group should not be buried too deeply in the membrane bilayer; and 3) to avoid perturbing structural features of the Chol molecule that are known to be critical for biological function, such as the isooctyl tail, the α-face, the 3β-hydroxy, and the $\Delta^{5(6)}$ double bond.[20]

We first asked if eChol could retain the biological properties of Chol in a stringent functional assay. M19 CHO cells are defective in Chol biosynthesis and require exogenous Chol for growth and proliferation.[21] Both Chol and eChol completely rescued the proliferation of M19 CHO cells grown in delipidated medium (Figure 1B); this indicates that eChol closely mimics the function of Chol in cells. We determined that a two-hour labeling pulse with eChol (12.5 μM) resulted in a cellular concentration of eChol that was 27% that of endogenous Chol (Figure S1A in the Supporting Information); thus, significant amounts of eChol can be rapidly delivered to cells.

We next asked if eChol was able to substitute for Chol in the Hh signaling pathway. Hh signaling is initiated by the secreted Hh ligand, which is synthesized as a precursor that undergoes Chol-dependent self-cleavage, resulting in an N-terminal fragment covalently attached to Chol (the Hh ligand) and a C-terminal fragment.[4] Chol modification of the Hh ligand is critical for normal Hh signaling.[5] In an in vitro Chol modification reaction with purified Hh precursor, eChol supported Hh self-cleavage as efficiently as Chol (Figure S1B), generating an eChol-modified N-terminal fragment, which could be specifically detected by CuAAC with biotin-azide followed by anti-biotin blotting (Figure S1C). When cells expressing human Sonic hedgehog (hShh) are depleted of sterols, Chol-dependent self-cleavage is inhibited;[22] this inhibition is completely reversed by eChol and Chol but not by epicholesterol (Figure S1D). These results show that eChol is an efficient Chol substitute in the Hh modification reaction, both in vitro and in vivo.

Sterols are required for the activation of the seven-spanner membrane protein Smo, which, in turn, is required for Hh signal transduction.[7] When Hh-responsive cells are depleted of sterols, Hh signaling is blocked; this inhibition is reversed in a dose-dependent manner by re-addition of Chol and eChol, but not by re-addition of epicholesterol (Figure 2A). Interestingly, eChol rescues Hh signaling at a significantly lower concentration than Chol (Figure 2A and experiments below); we speculate that the increased biological activity of eChol is due to increased solubility, which perhaps allows for more efficient delivery to cells. Hh stimulation leads to rapid recruitment of Smo to the primary cilium,[23] a critical step in Smo activation. In sterol-depleted cells, Smo fails to be recruited to cilia in response to Hh stimulation (Figure 2B), which provides a sufficient explanation as to why sterols are required for Hh signal transduction. Importantly, signal-dependent recruitment of Smo to cilia is rescued in sterol-depleted cells by addition of Chol and eChol, but not epicholesterol (Figure 2B–D). Thus, eChol can completely replace Chol to support signal-dependent recruitment of Smo to primary cilia and Hh signal transduction.

We next developed a method for imaging eChol in cells by CuAAC with a fluorescent azide. Surprisingly, several fluorescent azides (Figure S2) that strongly stain cells labeled with other alkyne probes (such as 5-ethynyl-2′-deoxyuridine, which incorporates into DNA,[24] or propargylcholine, which incorporates into phospholipids[25]) failed to stain eChol-labeled cells. We found, however, that fluorescein-azide and tetramethylrhodamine-picolyl azide (TMR-picolyl azide, Figure S2) allowed for robust and specific staining of eChol incorporated into cellular membranes (Figure 3A and B). Although we do not understand the basis for this differential reactivity, perhaps fluorescein-azide and TMR-picolyl azide, by virtue of their increased hydrophobicity, can access the ethynyl group of membrane-embedded eChol, whereas more the hydrophilic azides cannot. This interpretation is supported by the fact that azides that fail to stain eChol embedded in cellular membranes readily react with eChol covalently attached to the Hh ligand (Figures S1C and S2).

EChol staining is intense and uniform among cells, and its pattern is characteristic of Chol incorporation into cellular membranes (Figure 3A and B), including the plasma membrane and a large number of intracellular structures, both punctate and elongated in shape. Importantly, the eChol stain is excluded from inside the nucleus, which is devoid of mem-

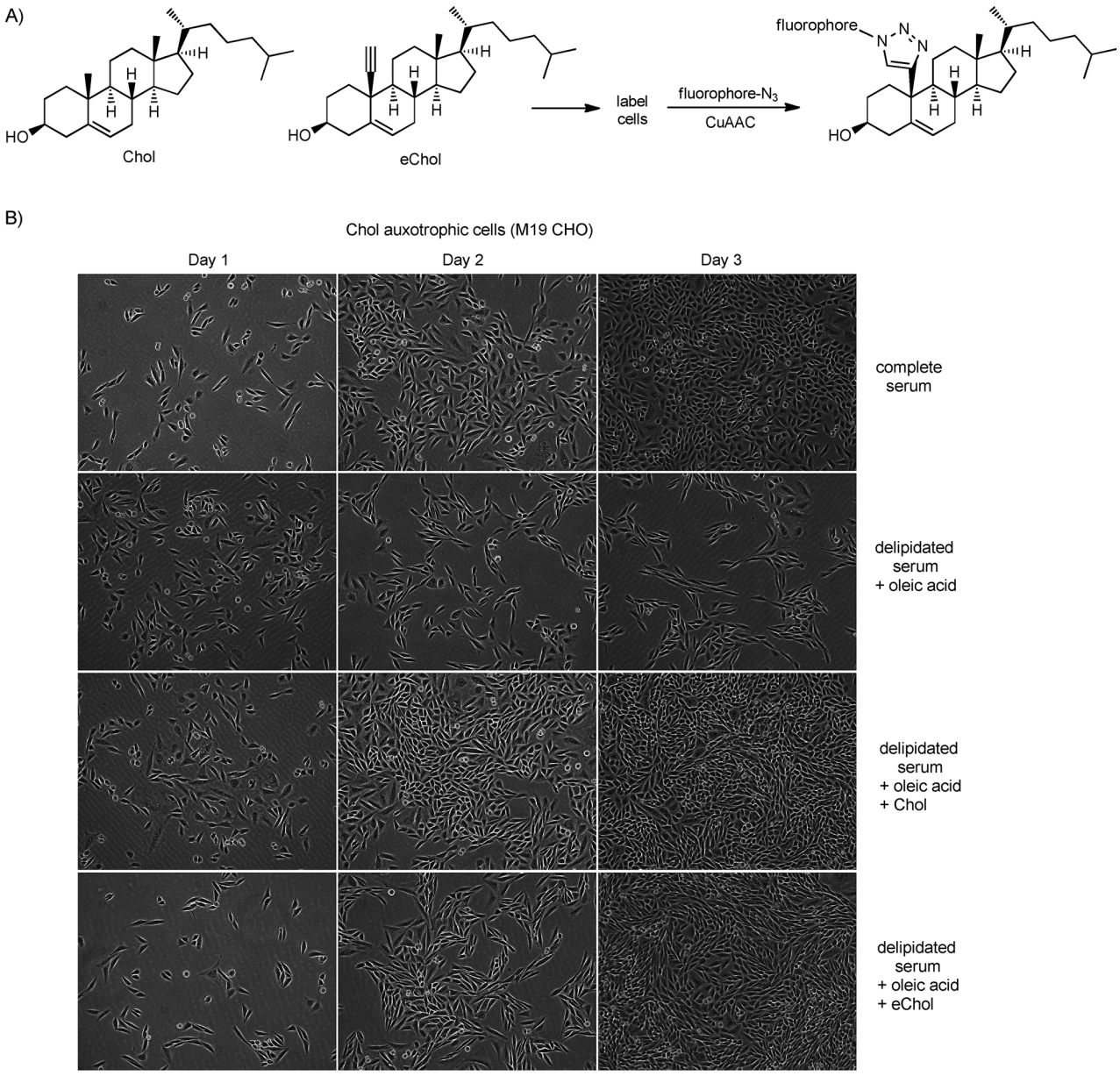

Figure 1. 19-Ethynylcholesterol (eChol) is a functional bioorthogonal analogue of cholesterol (Chol). A) Structures of cholesterol (Chol) and eChol, a Chol analogue in which a terminal alkyne group replaces the axial methyl at position C-19 of the sterol molecule. After labeling cells, eChol can be imaged by fluorescence microscopy, following copper(I)-catalyzed azide–alkyne cycloaddition (CuAAC) with fluorescein-azide. B) Chol auxotrophic M19 CHO cells were grown for 4 days in medium containing delipidated serum supplemented with oleic acid (35 μM) and in the presence or absence of Chol (10 μM) or eChol (35 μM), added as soluble methyl β-cyclodextrin (MCD) complexes. Representative fields of cells were photographed on days 1, 2, and 3 after plating. M19 CHO cells cannot proliferate in the absence of sterols; any proliferation was completely rescued by eChol or Chol.

branes. EChol staining is sensitive to detergents (Figure S3), consistent with a non-covalent interaction between eChol and the membrane bilayer.

We examined the subcellular distribution of eChol in more detail by co-localizing the eChol stain with red fluorescent protein (RFP) fusions that mark specific cellular membranes or organelles. Cultured cells were transiently transfected with plasmids encoding RFP fusions targeted to the plasma membrane, endoplasmic reticulum (ER), or mitochondria, and were then labeled with eChol, followed by staining with fluorescein-azide (Figure 3C). The highest eChol levels were found in mitochondria, with significantly lower eChol localization to the ER (compare bottom and middle panels in Figure 3C), consistent with the low levels of Chol normally found in ER membranes.[26] EChol also localized to the plasma membrane (Figure 3C and D). As cells maintain Chol at different levels in different cellular membranes, eChol will be a useful tool for imaging the subcellular distribution of Chol.

In some experiments, it would be desirable to image simultaneously both Chol and another lipid component of membranes. We exploited the differential reactivity of eChol towards fluorescent azides to image the subcellular distribution

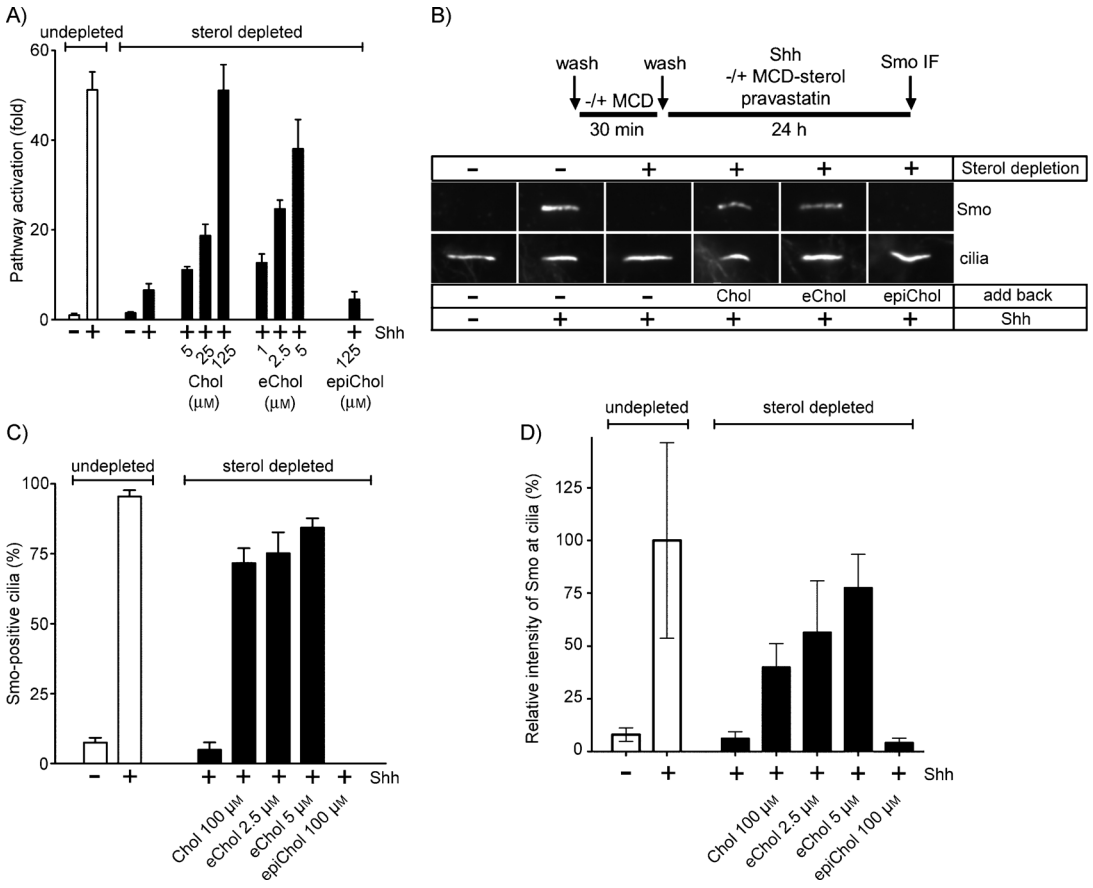

Figure 2. EChol supports efficient Hedgehog (Hh) signal transduction. A) Hh-responsive NIH-3T3 Shh-LightII cells[31] were sterol-depleted with MCD, followed by re-addition of sterol for 1 h as sterol–MCD complexes. The cells were then incubated overnight with Shh and pravastatin (20 μM), followed by luciferase reporter assays. Relative luciferase counts were normalized to those of the undepleted and unstimulated cells. Error bars represent the standard deviation of the mean for four independent experiments. The Hh pathway activity is inhibited by sterol depletion, which can be reversed in a dose-dependent manner by Chol or eChol, but not by the diastereomer, epicholesterol. B) NIH-3T3 cells were depleted of sterols, as in (A), and were incubated overnight with Shh and pravastatin (20 μM) in the absence or presence of MCD complexes of Chol, epicholesterol, or eChol. Undepleted cells, stimulated or not stimulated with Shh, were used as controls. The cells were processed for immunofluorescence for Smoothened (Smo) and acetylated tubulin (primary cilia marker). Representative micrographs of Smo localization to cilia are shown. Sterol depletion blocks recruitment of Smo to cilia in response to Shh stimulation; this effect was reversed by Chol and eChol, but not by epicholesterol. C) Quantification of Smo-positive cilia for the experiment in (B). Error bars represent the standard deviation of the mean for three groups of at least 50 cilia each, scored visually for the presence or absence of Smo. D) Quantification of Smo fluorescence intensity at primary cilia for the experiment in (B), normalized to the fluorescence of Smo in cilia of undepleted, Shh-stimulated cells. Error bars represent the standard deviation of the mean relative Smo intensity ($n > 100$ cilia per condition).

of eChol and choline phospholipids, the most abundant lipids in cellular membranes (Figure 4). Choline phospholipids were metabolically labeled with propargylcholine (PCho) and were detected by CuAAC with a fluorescent azide (Alexa568-azide) that does not react with eChol in membranes, followed by detection of eChol with fluorescein-azide. The bioorthogonal detection of choline phospholipids and eChol is sensitive and specific, allowing imaging by high-resolution fluorescence microscopy of both of these lipids in membranes. Thus, successive use of a CuAAC reaction with different fluorescent azides can accomplish two-color imaging of two alkyne-tagged lipids in cells.

As alkyne tagging of the C-19 position proved a good choice for preserving the biological function of Chol, we extended this approach to oxysterols, a class of oxygenated Chol derivatives whose potent biological effects are still poorly understood. We focused on 25-hydroxycholesterol (25-OHC, Figure 5A), as it is one of the most abundant oxysterols in vivo and has been implicated in numerous biological processes.[27] We synthesized the alkyne analogue 19-ethynyl-25-hydroxycholesterol (25-OH-eChol, Figure 5A). Gratifyingly, 25-OH-eChol retained the potent stimulatory effect of oxysterols on the Hh pathway, as determined by recruitment of Smo to primary cilia (Figure 5B), by activation of an Hh-responsive luciferase reporter (Figure 5C), and by transcription of endogenous target genes (Figure 5D). Importantly, Hh activation by 25-OH-eChol was blocked by the small molecule Smo inhibitor, SANT1 (Figure S4), indicating that 25-OH-eChol acted at the level of Smo, as expected for Hh-activating oxysterols.[28] Interestingly, 25-OH-eChol appeared slightly more potent than 25-OHC (Figure 5D), similar to the higher biological activity of eChol compared to Chol (see above, Figure 2), perhaps due to increased solubility. Finally, using the CuAAC protocol developed for eChol allowed robust imaging of 25-OH-eChol in cells, reveal-

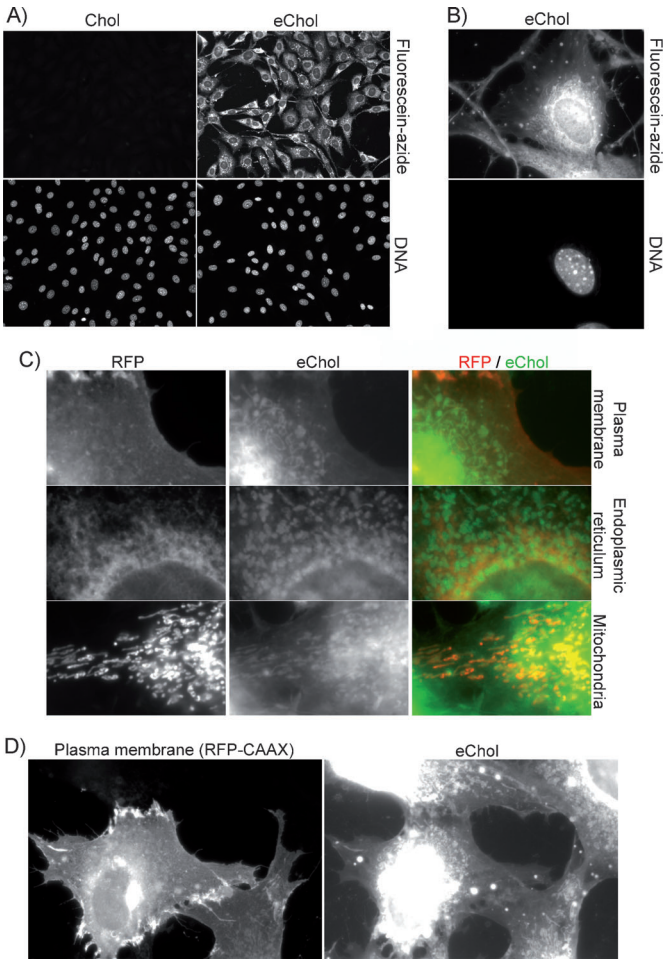

Figure 3. Using eChol as an imaging probe for microscopic detection of Chol in cells. A) NIH-3T3 cells, incubated for 12 h with or without eChol (20 μM from DMSO stock), were stained by CuAAC with fluorescein-azide and by Hoechst and were then imaged by fluorescence microscopy. The eChol staining pattern is characteristic of incorporation into various cellular membranes. B) Higher magnification view of a cell labeled with eChol and stained with fluorescein-azide. C) Subcellular distribution of eChol. NIH-3T3 cells were transiently transfected with plasmids expressing red fluorescent protein (RFP) fusions targeted to various cellular membranes: plasma membrane (pmCherry-CAAX plasmid), endoplasmic reticulum (ER; pmCherry-Sec61β plasmid), and mitochondria (pDsRed-Mito plasmid). The cells were then labeled with eChol and stained with fluorescein-azide as in (A). Left: RFP images; center: eChol images; right: overlay of RFP (red) and eChol (green). EChol appears enriched in mitochondria relative to the ER (compare bottom and middle), consistent with the low levels of Chol normally found in ER. EChol also co-localizes with the plasma membrane marker (top). D) As in (C), but showing a high magnification view of eChol co-localization with the plasma membrane marker, mCherry-CAAX. Left panel: mCherry-CAAX image; right panel: eChol image. The two cells at the bottom of the micrographs expressed mCherry-CAAX, whereas the two top cells did not.

ing its localization to various cellular membranes (Figure 5E and F); thus, 25-OH-eChol will be a useful probe for imaging 25-OHC distribution in cells and organelles with high sensitivity and spatial resolution.

Experimental Section

NIH-3T3 cells were labeled by incubation with eChol (added from stocks in DMSO or as soluble MCD complexes) or 25-OH-eChol

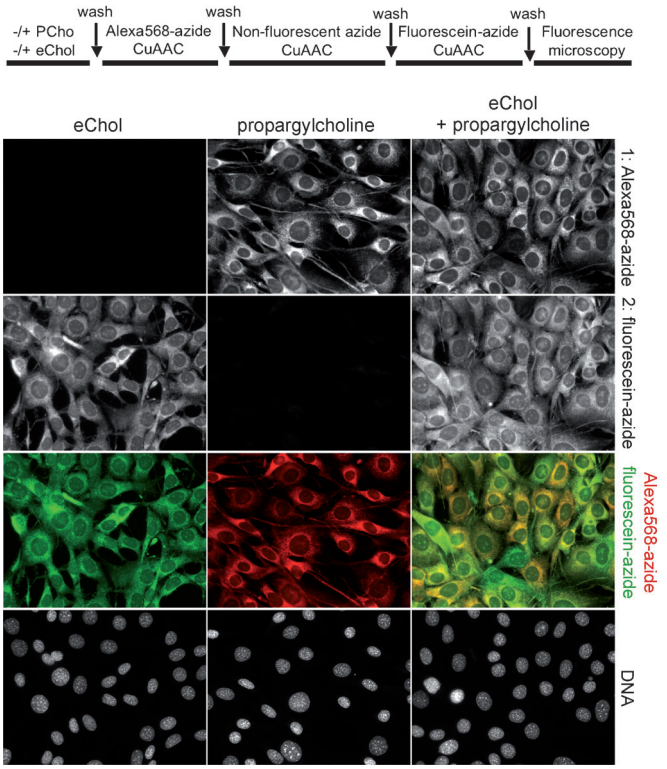

Figure 4. Double labeling and two-color imaging of Chol and phospholipids in cells. NIH-3T3 cells were incubated overnight with propargylcholine (PCho, 100 μM) to label choline phospholipids, after which they were incubated overnight in the absence or presence of eChol (40 μM from DMSO stock). EChol in cellular membranes reacts with fluorescein-azide but not with Alexa568-azide (Figure S2); this differential reactivity was used to achieve two-color imaging of eChol- and PCho-labeled phospholipids. The labeled cells were first stained with Alexa568-azide (to detect PCho), after which the unreacted PCho phospholipids were consumed by reaction with excess non-fluorescent azide. Finally, the cells were stained with fluorescein-azide (to detect eChol). Top row: PCho-labeled phospholipids; second row: eChol; third row: overlay of PCho (red) and eChol (green) images; bottom row: Hoechst staining of cell nuclei.

(added from stocks in DMSO) in DMEM. The cells were fixed with 3.7% formaldehyde in PBS, washed with Tris-buffered saline (TBS, 10 mM Tris·HCl, 150 mM NaCl, pH 7.5), reacted by CuAAC with fluorescein-azide (10 μM) as described,[24] and then washed several times with NaCl (0.5 M) and TBS (to remove the unreacted azide). Cells were imaged by epi-fluorescence microscopy on a Nikon TE2000U microscope equipped with an OrcaER digital camera (Hammamatsu) and 20x PlanApo 0.75NA, 40x PlanApo 0.95NA, or 100x PlanApo 1.4NA objectives (Nikon). For imaging subcellular localization of eChol, cells were transiently transfected by using polyethyleneimine, with plasmids encoding RFP fusions targeted to mitochondria (pDsRed-Mito plasmid from Clontech Laboratories Inc), the endoplasmic reticulum (pmCherry-Sec61β, plasmid #49155 from Addgene), or the plasma membrane (pmCherry-CAAX plasmid[29]). After transfection, the cells were labeled with eChol and stained and imaged as described above.

For double labeling experiments, cells were first labeled overnight with propargylcholine (PCho, 100 μM) and then overnight with eChol (40 μM, added from DMSO stock). The cells were stained first by CuAAC with Alexa568-azide (10 μM) to detect PCho-labeled phospholipids.[25] The PCho-labeled phospholipids left unreacted after reaction with Alexa568-azide were consumed by performing

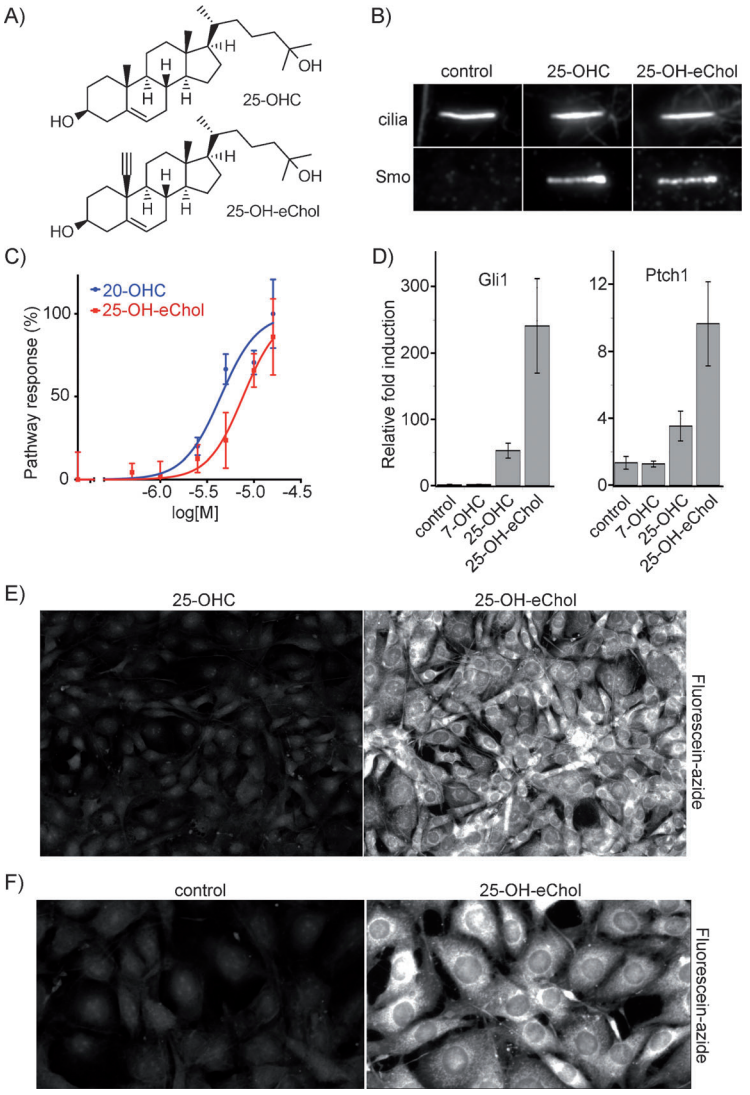

Figure 5. A bioorthogonal oxysterol probe. A) Structure of the oxysterol, 25-hydroxycholesterol (25-OHC), and of the alkyne 25-OHC analogue, 19-ethynyl-25-hydroxycholesterol (25-OH-eChol). B) NIH-3T3 cells were treated overnight with 25-OHC or 25-OH-eChol (each at 10 μM), and localization of endogenous Smo to primary cilia was determined by immunofluorescence. Primary cilia were labeled with antibodies against acetylated tubulin. Both 25-OHC and 25-OH-eChol cause Smo to accumulate at cilia, a hallmark of Hh pathway activation. C) Hh-responsive Shh-LightII cells were treated with varying concentrations of 25-OH-eChol or 20(*s*)-hydroxycholesterol (20-OHC, the most potent Hh-activating oxysterol), and activation of the Hh pathway was measured by luciferase assay. Error bars represent standard deviation ($n=4$ independent experiments). 25-OH-eChol activates Hh signaling, with an EC_{50} comparable to that of 20-OHC. D) Confluent cultures of NIH-3T3 cells were incubated overnight in serum-free medium, in the absence or presence of the indicated oxysterols (10 μM each), and transcription of Gli1 and Ptch1, two targets of the Hh pathway, was measured by quantitative RT-PCR (qPCR). Error bars show standard deviation ($n=3$ independent experiments). The oxysterol, 7-hydroxycholesterol (7-OHC), is inactive in Hh signaling and was used as negative control. 25-OH-eChol potently activates transcription of Hh target genes. E) NIH-3T3 cells were incubated for 12 h with 25-OHC or 25-OH-eChol (10 μM each) and were then stained with fluorescein-azide by CuAAC, followed by fluorescence microscopy imaging. Cells labeled with 25-OH-eChol showed strong, specific staining. F) As in (E), but showing a higher magnification image. 25-OH-eChol shows a staining pattern indicative of its broad distribution in cellular membranes.

a subsequent CuAAC reaction with *O*-(2-aminoethyl)-*O*′-(2-azidoethyl)-pentaethylene glycol (5 mM), as described.[25] The cells were then washed and reacted with fluorescein-azide (10 μM) to detect eChol.

To test if eChol rescues proliferation of Chol auxotrophic CHO M19 cells, the cells were grown for four days in medium supplemented with 10% delipidated serum and oleic acid (35 μM), in the absence or presence of eChol (10 μM) or Chol (35 μM), both added as soluble MCD complexes. Representative fields of cells were photographed at 24 h intervals on days 1, 2, and 3 after plating by phase contrast microscopy.

To deplete sterols from NIH-3T3 cells, cultures were starved overnight and were then incubated with MCD in DMEM (1% *w*/*v*) for 30 min. For rescue experiments, sterols were added back as sterol–MCD complexes in DMEM supplemented with pravastatin (20 μM). To assay the effect of sterol depletion on Hh stimulation, the Hh ligand was added to the depleted cells in DMEM with pravastatin, with or without sterol–MCD complexes. Undepleted cells, stimulated or not stimulated with Hh ligand, served as positive and negative controls. The cells were processed for Smo immunofluorescence or for luciferase assays, as described above.

Activity assays for Hh signaling were performed in NIH-3T3 cells. Confluent cell cultures were starved for 24 h in medium without serum and were then stimulated with Hh ligand. After the desired amount of time, the cultures were analyzed by either immunofluorescence (to determine recruitment of Smo to primary cilia), by luciferase reporter assays, or by quantitative PCR (qPCR; to measure the transcriptional output of the Hh pathway).

Smo immunofluorescence was performed with rabbit anti-Smo antibodies, as described.[30] Primary cilia were stained with a mouse anti-acetylated tubulin monoclonal antibody (Sigma). For each condition, the presence or absence of Smo at cilia was scored visually for 150 cilia. Error bars represent the standard deviation of the mean for groups of 50 cilia counted on different visual fields on the same coverslip. All experiments showing ciliary counts were repeated independently at least three times. To measure Smo fluorescence intensity, the primary cilium was outlined by using acetylated tubulin images, and the integrated ciliary intensity for Smo was measured by using Metamorph software (Applied Precision).

Luciferase reporter assays were performed in NIH-3T3 Shh-LightII cells, which express firefly luciferase under the control of an artificial Hh-responsive promoter and Renilla luciferase under the control of a constitutive promoter, as described.[31] The activity of the Hh pathway was calculated as the ratio between firefly and Renilla luciferase activities after background subtraction. Error bars represent the standard deviation of the mean for four independent experiments.

Hh-stimulated transcription of the target genes, Gli1 and Ptch1, was measured by qPCR in NIH-3T3 cells, as described.[32] Each qPCR experiment was performed in triplicate starting from three biological samples, and error bars represent standard deviation.

Acknowledgements

We thank T.Y. Chang (Dartmouth) for M19 CHO cells and Carlos Gartner for advice on sterol chemistry. C.Y.J. was supported by a National Science Foundation (NSF) fellowship. This work was supported in part by National Institutes of Health (NIH) R01 grants GM092924 and GM110041.

The authors declare no competing financial interests.

Keywords: cholesterol · click chemistry · Hedgehog signaling · membranes · microscopy

[1] F. R. Maxfield, G. van Meer, *Curr. Opin. Cell Biol.* **2010**, *22*, 422 – 429.
[2] a) T. Y. Chang, C. C. Chang, N. Ohgami, Y. Yamauchi, *Annu. Rev. Cell Dev. Biol.* **2006**, *22*, 129 – 157; b) B. Mesmin, F. R. Maxfield, *Biochim. Biophys. Acta Mol. Cell Biol. Lipids* **2009**, *1791*, 636 – 645; c) J. L. Goldstein, R. A. DeBose-Boyd, M. S. Brown, *Cell* **2006**, *124*, 35 – 46.
[3] a) J. Taipale, P. A. Beachy, *Nature* **2001**, *411*, 349 – 354; b) M. M. Cohen, Jr., *Am. J. Med. Gen. Part A* **2003**, *123*, 5 – 28; c) L. Lum, P. A. Beachy, *Science* **2004**, *304*, 1755 – 1759.
[4] J. A. Porter, K. E. Young, P. A. Beachy, *Science* **1996**, *274*, 255 – 259.
[5] a) T. Maity, N. Fuse, P. A. Beachy, *Proc. Natl. Acad. Sci. USA* **2005**, *102*, 17026 – 17031; b) E. Roessler, K. B. El-Jaick, C. Dubourg, J. I. Velez, B. D. Solomon, D. E. Pineda-Alvarez, F. Lacbawan, N. Zhou, M. Ouspenskaia, A. Paulussen, H. J. Smeets, U. Hehr, C. Bendavid, S. Bale, S. Odent, V. David, M. Muenke, *Human Mutation* **2009**, *30*, E921 – 935.
[6] a) J. Alcedo, M. Ayzenzon, T. Von Ohlen, M. Noll, J. E. Hooper, *Cell* **1996**, *86*, 221 – 232; b) M. van den Heuvel, P. W. Ingham, *Nature* **1996**, *382*, 547 – 551.
[7] M. K. Cooper, C. A. Wassif, P. A. Krakowiak, J. Taipale, R. Gong, R. I. Kelley, F. D. Porter, P. A. Beachy, *Nat. Genet.* **2003**, *33*, 508 – 513.
[8] S. Nachtergaele, L. K. Mydock, K. Krishnan, J. Rammohan, P. H. Schlesinger, D. F. Covey, R. Rohatgi, *Nat. Chem. Biol.* **2012**, *8*, 211 – 220.
[9] a) D. Nedelcu, J. Liu, Y. Xu, C. Jao, A. Salic, *Nat. Chem. Biol.* **2013**, *9*, 557 – 564; b) S. Nachtergaele, D. M. Whalen, L. K. Mydock, Z. Zhao, T. Malinauskas, K. Krishnan, P. W. Ingham, D. F. Covey, C. Siebold, R. Rohatgi, *eLife* **2013**, *2*, e01340; c) B. R. Myers, N. Sever, Y. C. Chong, J. Kim, J. D. Belani, S. Rychnovsky, J. F. Bazan, P. A. Beachy, *Dev. Cell* **2013**, *26*, 346 – 357.
[10] A. Chattopadhyay, E. London, *Biochim. Biophys. Acta Biomembr.* **1988**, *938*, 24 – 34.
[11] M. R. Alecio, D. E. Golan, W. R. Veatch, R. R. Rando, *Proc. Natl. Acad. Sci. USA* **1982**, *79*, 5171 – 5174.
[12] M. Mondal, B. Mesmin, S. Mukherjee, F. R. Maxfield, *Mol. Biol. Cell* **2008**, *20*, 581 – 588.
[13] a) S. Mukherjee, X. Zha, I. Tabas, F. R. Maxfield, *Biophys. J.* **1998**, *75*, 1915 – 1925; b) A. L. McIntosh, B. P. Atshaves, H. Huang, A. M. Gallegos, A. B. Kier, F. Schroeder, *Lipids* **2008**, *43*, 1185 – 1208; c) D. Wüstner, *Chem. Phys. Lipids* **2007**, *146*, 1 – 25.
[14] a) O. Beknke, J. Tranum-Jensen, B. van Deurs, *Eur. J. Cell Biol.* **1984**, *35*, 189 – 199; b) O. Behnke, J. Tranum-Jensen, B. van Deurs, *Eur. J. Cell Biol.* **1984**, *35*, 200 – 215.
[15] S. Nishimura, K. Ishii, K. Iwamoto, Y. Arita, S. Matsunaga, Y. Ohno-Iwashita, S. B. Sato, H. Kakeya, T. Kobayashi, M. Yoshida, *PloS One* **2013**, *8*, e83716.
[16] M. Iwamoto, I. Morita, M. Fukuda, S. Murota, S. Ando, Y. Ohno-Iwashita, *Biochim. Biophys. Acta Biomembr.* **1997**, *1327*, 222 – 230.
[17] K. Hofmann, C. Thiele, H. F. Schott, A. Gaebler, M. Schoene, Y. Kiver, S. Friedrichs, D. Lutjohann, L. Kuerschner, *J. Lipid Res.* **2014**, *55*, 583 – 591.
[18] a) C. W. Tornøe, C. Christensen, M. Meldal, *J. Org. Chem.* **2002**, *67*, 3057 – 3064; b) V. V. Rostovtsev, L. G. Green, V. V. Fokin, K. B. Sharpless, *Angew. Chem. Int. Ed.* **2002**, *41*, 2596 – 2599; *Angew. Chem.* **2002**, *114*, 2708 – 2711.
[19] a) J. Kalvoda, G. Anner, *Helv. Chim. Acta* **1967**, *50*, 269 – 281; b) M. S. Mathai, R. A. Pascal, Jr., *Steroids* **1994**, *59*, 244 – 247.
[20] K. Bloch, *Steroids* **1989**, *53*, 261 – 270.
[21] J. S. Limanek, J. Chin, T. Y. Chang, *Proc. Natl. Acad. Sci. USA* **1978**, *75*, 5452 – 5456.
[22] R. K. Guy, *Proc. Natl. Acad. Sci. USA* **2000**, *97*, 7307 – 7312.
[23] a) K. C. Corbit, P. Aanstad, V. Singla, A. R. Norman, D. Y. Stainier, J. F. Reiter, *Nature* **2005**, *437*, 1018 – 1021; b) R. Rohatgi, L. Milenkovic, M. P. Scott, *Science* **2007**, *317*, 372 – 376.
[24] A. Salic, T. J. Mitchison, *Proc. Natl. Acad. Sci. USA* **2008**, *105*, 2415 – 2420.
[25] C. Y. Jao, M. Roth, R. Welti, A. Salic, *Proc. Natl. Acad. Sci. USA* **2009**, *106*, 15332 – 15337.
[26] A. Radhakrishnan, J. L. Goldstein, J. G. McDonald, M. S. Brown, *Cell Metab.* **2008**, *8*, 512 – 521.
[27] U. Diczfalusy, *Biochimie* **2013**, *95*, 455 – 460.
[28] a) R. B. Corcoran, M. P. Scott, *Proc. Natl. Acad. Sci. USA* **2006**, *103*, 8408 – 8413; b) J. R. Dwyer, N. Sever, M. Carlson, S. F. Nelson, P. A. Beachy, F. Parhami, *J. Biol. Chem.* **2007**, *282*, 8959 – 8968.
[29] L. Lu, M. S. Ladinsky, T. Kirchhausen, *J. Cell Biol.* **2011**, *194*, 425 – 440.
[30] H. Tukachinsky, L. Lopez, A. Salic, *J. Cell Biol.* **2010**, *191*, 415 – 428.
[31] J. Taipale, J. K. Chen, M. K. Cooper, B. Wang, R. K. Mann, L. Milenkovic, M. P. Scott, P. A. Beachy, *Nature* **2000**, *406*, 1005 – 1009.
[32] H. Tukachinsky, L. V. Lopez, A. Salic, *J. Cell Biol.* **2010**, *191*, 415 – 428.

Received: April 16, 2014
Revised: December 23, 2014
Published online on February 6, 2015